Article

# Formation and Stabilization Model of the 42-mer Aβ Radical: Implications for the Long-Lasting Oxidative Stress in Alzheimer's Disease

Kazuma Murakami, Kazuhiro Irie, Hajime Ohigashi, Hideyuki Hara, Masaya Nagao, Takahiko Shimizu, and Takuji Shirasawa

*J. Am. Chem. Soc.*, **2005**, 127 (43), 15168-15174• DOI: 10.1021/ja054041c • Publication Date (Web): 11 October 2005



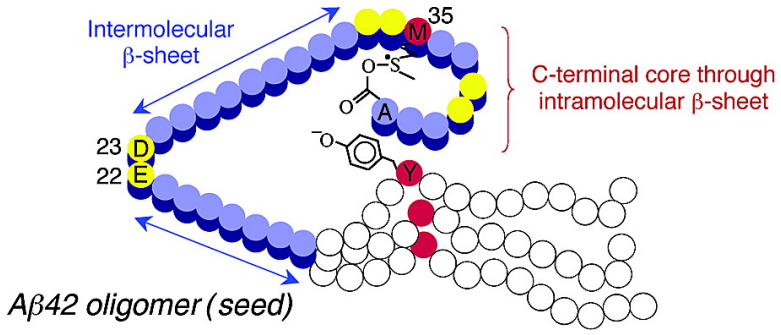


## More About This Article

Additional resources and features associated with this article are available within the HTML version:

- Supporting Information
- Links to the 5 articles that cite this article, as of the time of this article download
- Access to high resolution figures
- Links to articles and content related to this article
- Copyright permission to reproduce figures and/or text from this article

View the Full Text HTML



Journal of the American Chemical Society is published by the American Chemical Society. 1155 Sixteenth Street N.W., Washington, DC 20036

J|A|C|S
ARTICLES
Published on Web 10/11/2005

# Formation and Stabilization Model of the 42-mer A$\beta$ Radical: Implications for the Long-Lasting Oxidative Stress in Alzheimer's Disease

Kazuma Murakami,[†] Kazuhiro Irie,*[,†] Hajime Ohigashi,[†] Hideyuki Hara,[‡] Masaya Nagao,[§] Takahiko Shimizu,[||] and Takuji Shirasawa[||]

*Contribution from the Division of Food Science and Biotechnology, Graduate School of Agriculture, Kyoto University, Kyoto 606-8502, Japan, Division of ESR, Bruker Biospin K. K., Ibaraki 305-0051, Japan, Division of Integrated Life Science, Graduate School of Biostudies, Kyoto University, Kyoto 606-8502, Japan, and Research Team for Molecular Biomarkers, Tokyo Metropolitan Institute of Gerontology, Tokyo 173-0015, Japan*

Received June 18, 2005; E-mail: irie@kais.kyoto-u.ac.jp

***Abstract:*** Amyloid fibrils mainly consist of 40-mer and 42-mer peptides (A$\beta$40, A$\beta$42). A$\beta$42 is believed to play a crucial role in the pathogenesis of Alzheimer's disease because its aggregative ability and neurotoxicity are considerably greater than those of A$\beta$40. The neurotoxicity of A$\beta$ peptides involving the generation of free radicals is closely related to the *S*-oxidized radical cation of Met-35. However, the cation's origin and mechanism of stabilization remain unclear. Recently, structural models of fibrillar A$\beta$42 and A$\beta$40 based on systematic proline replacement have been proposed by our group [Morimoto, A.; et al. *J. Biol. Chem.* **2004**, *279*, 52781] and Wetzel's group [Williams, A. D.; et al. *J. Mol. Biol.* **2004**, *335*, 833], respectively. A major difference between these models is that our model of A$\beta$42 has a C-terminal $\beta$-sheet region. Our biophysical study on A$\beta$42 using electron spin resonance (ESR) suggests that the *S*-oxidized radical cation of Met-35 could be generated by the reduction of the tyrosyl radical at Tyr-10 through a turn structure at positions 22 and 23, and stabilized by a C-terminal carboxylate anion through an intramolecular $\beta$-sheet at positions 35−37 and 40−42 to form a C-terminal core that would lead to aggregation. A time-course analysis of the generation of radicals using ESR suggests that stabilization of the radicals by aggregation might be a main reason for the long-lasting oxidative stress of A$\beta$42. In contrast, the *S*-oxidized radical cation of A$\beta$40 is too short-lived to induce potent neurotoxicity because no such stabilization of radicals occurs in A$\beta$40.

## Introduction

Alzheimer's disease (AD) and cerebral amyloid angiopathy (CAA) are generally characterized by the progressive deposition of amyloid fibrils.[1] The deposits are mainly composed of 40- and 42-mer peptides (A$\beta$40 and A$\beta$42) produced from amyloid precursor protein by two proteases, $\beta$- and $\gamma$-secretase.[2,3] A$\beta$42 is considered to play a pivotal role in the pathogenesis of AD because it shows greater aggregative ability and neurotoxicity than A$\beta$40.[4]

AD and CAA are associated with increased oxidative stress.[5,6] There is considerable evidence that A$\beta$ damages neurons through the Cu(II)-catalyzed reduction of molecular oxygen to hydrogen peroxide ($H_2O_2$), and that both the tyrosyl radical at position 10 and the *S*-oxidized radical cation of Met-35 are critical for the neurotoxicity.[7,8] These radical species are too short-lived to cause neurotoxic damage continuously. Recent research using a surrogate peptide of A$\beta$42 (A$\beta$25−35)[9] with neurotoxicity indicated that the C-terminal carboxylate anion of Met-35 stabilizes the *S*-oxidized radical cation by forming a six-membered ring via an intramolecular S−O bond as reported in the *N*-acetylmethionine amide.[10] Several stabilization mechanisms in the case of full-length A$\beta$42 have also been proposed.[11,12] However, the mechanism behind the stabilization of the A$\beta$42 radical at Met-35, which may explain the large difference in aggregative ability and neurotoxicity between A$\beta$42 and A$\beta$40, remains to be elucidated.

[†] Graduate School of Agriculture, Kyoto University.
[‡] Bruker Biospin K. K.
[§] Graduate School of Biostudies, Kyoto University.
[||] Tokyo Metropolitan Institute of Gerontology.

(1) Selkoe, D. J. *Trends Cell Biol.* **1998**, *8*, 447−453.
(2) Iwatsubo, T.; Odaka, A.; Suzuki, N.; Mizusawa, H.; Nukina, N.; Ihara, Y. *Neuron* **1994**, *13*, 45−53.
(3) Iwatsubo, T.; Mann, D. M. A.; Odaka, A.; Suzuki, N.; Ihara, Y. *Ann. Neurol.* **1995**, *37*, 294−299.
(4) Davis, J.; van Nostrand, W. E. *Proc. Natl. Acad. Sci. U.S.A.* **1996**, *93*, 2996−3000.
(5) Butterfield, D. A. *Curr. Med. Chem.* **2003**, *10*, 2651−2659.
(6) Bush, A. I. *Trends Neurosci.* **2003**, *26*, 207−214.
(7) Varadarajan, S.; Yatin, S.; Kanski, J.; Jahanshahi, F.; Butterfield, D. A. *Brain Res. Bull.* **1999**, *50*, 133−141.
(8) Atwood, C. S.; Perry, G.; Zeng, H.; Kato, Y.; Jones, W. D.; Ling, K.-Q.; Huang, X.; Moir, R. D.; Wang, D.; Sayre, L. M.; Smith, M. A.; Chen, S. G.; Bush, A. I. *Biochemistry* **2004**, *43*, 560−568.
(9) Varadarajan, S.; Kanski, J.; Aksenova, M.; Lauderback, C.; Butterfield, D. A. *J. Am. Chem. Soc.* **2001**, *123*, 5625−5631.
(10) Schöneich, C.; Pogocki, D.; Wisniowski, P.; Hug, G. L.; Bobrowski, K. *J. Am. Chem. Soc.* **2000**, *122*, 10224−10225.
(11) Varadarajan, S.; Yatin, S.; Aksenova, M.; Butterfield, D. A. *J. Struct. Biol.* **2000**, *130*, 184−208.


**10.1021/ja054041c CCC: $30.25** 

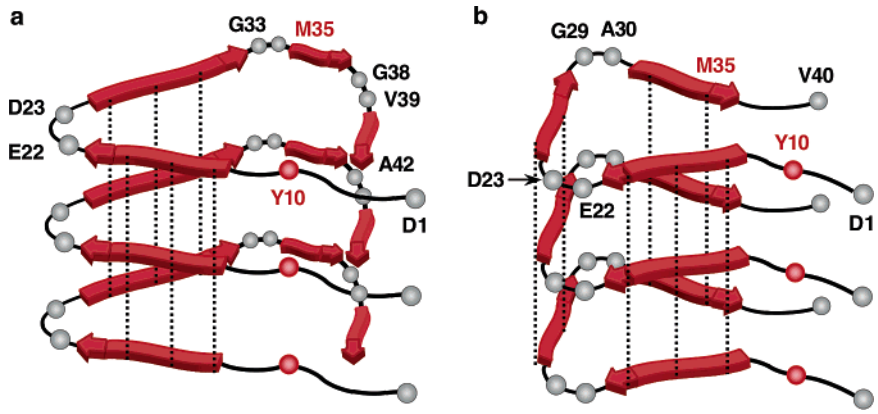


***Figure 1.*** The structural models of Aβ fibrils deduced from the systematic replacement of prolines. (a) Aβ42 by our group[15] and (b) Aβ40 by Wetzel and colleagues.[16] The dotted lines indicate hydrogen bonds.

The replacement of prolines in peptides is a promising and rapid method of predicting secondary structure, especially a β-sheet and a turn. Prolines occur rarely in β-sheets, while they are easily accommodated in a turn such as a Pro−X corner.[13] This concept was first applied to structural studies using Aβ fragments (Aβ15−23 and Aβ12−26)[14] and I31P−Aβ42.[12] Recently, structural models of fibrillar Aβ42 (Figure 1a)[15] and Aβ40 (Figure 1b)[16] have been proposed on the basis of a systematic replacement with proline in full-length Aβ peptides by us and Williams et al., respectively. Both of these models have a turn structure at positions 22 and 23 related to the mutations in CAA, but differ in the structure of the C-terminal region. Our recent studies[17,18] revealed that the CAA-related mutants of Aβ42 and Aβ40 altered at position 22 [E22K (Italian), E22Q (Dutch), and E22G (Arctic)], which have a propensity to form a β-turn,[13] along with the E22P mutants showed 10−30 times stronger neurotoxicity than the corresponding wild-type Aβ peptide, while E22V−Aβ42 (valine as a β-turn breaker) did not show any neurotoxicity. These results suggest that the turn at positions 22 and 23 plays a critical role in the neurotoxicity of Aβ42 and Aβ40.

A major difference between the Aβ42 and Aβ40 aggregation models is that our model of Aβ42 adopts a C-terminal β-sheet structure even though it is not clear whether it is intermolecular or intramolecular. Previous NMR studies using Aβ42[19] or Aβ40[19,20] in the water-micelle condition suggest that the C-terminal structure could form an α-helix. In contrast, Tycko's group performed a solid-state NMR analysis of Aβ40 fibrils and found that C-terminal residues adopt an intermolecular β-sheet structure.[21−23] There seems to be a large difference in structure between the solid and the water-micelle states. We focused on the C-terminal structure at positions 35−42 to explain the stabilization of the Aβ42 radical at Met-35 because the C-terminal two residues are critical to the potent aggregative ability and neurotoxicity of Aβ42 as compared to Aβ40. This paper describes a comprehensive study on the ability to produce radicals, neurotoxicity, and aggregative ability of a series of Aβ42 mutants altered at positions 10, 22, 35, 38, and 42. The results led us to propose a new model for the aggregation of Aβ42 that can explain the mechanism behind the stabilization of the *S*-oxidized radical cation of Met-35 (Figure 4).

## Materials and Methods

**General.** The following spectroscopic and analytical instruments were used: ESR, Bruker EMX spectrometer; peptide synthesizer, Pioneer peptide synthesizer (Applied Biosystems, Foster City, CA); UV, Shimadzu UV-2200A; micro-plate reader, MPR-A4*i*II (TOSOH, Tokyo, Japan); HPLC, Waters 600E multisolvent delivery system with 2487 UV dual λ absorbance detector, and Waters 625 LC system with 486 UV tunable absorbance detector and 741 data module; matrix-assisted laser desorption/ionization time-of-flight mass spectrometry (MALDI-TOF-MS), Applied Biosystems Voyager-DE PRO. MALDI-TOF-MS was measured as reported previously.[24] HPLC was carried out on a Develosil-packed column ODS-UG-5 (20-mm inner diameter × 150 mm and 6.0-mm inner diameter × 100 mm) (Nomura Chemicals, Seto, Japan).

Chelex 100 resin, deferoxamine mesylate, and 3-(4,5-dimethylthiazol-2-yl)-2,5-diphenyltetrazolium bromide (MTT) reagent were purchased from Sigma. Phenyl-*tert*-butylnitrone (PBN) from Aldrich was purified by repeated recrystallization in ethyl acetate/hexane. BIOXYTECH $H_2O_2$-560 and Micro BCA protein assay kits were obtained from OXIS (Portland, OR) and Pierce (Rockford, IL), respectively. *N*-[(Dimethylamino)-1*H*-1,2,3-triazolo[4,5-*b*]pyridin-1-ylmethylene]-*N*-methylmethanaminium hexafluorophosphate *N*-oxide (HATU),[25] piperidine, Fmoc amino acids, Fmoc-Ala-PEG-PS (poly(ethylene glycol)-polystylene) resin, and *N*,*N*-diisopropylethylamine were purchased from Applied Biosystems. *N*,*N*-Dimethylformamide, trifluoroacetic acid, 1,2-ethanedithiol, thioanisole, *m*-cresol, and diethyl ether (peroxide-free) were purchased from Nacalai tesque (Kyoto, Japan).

(12) Kanski, J.; Aksenova, M.; Schöneich, C.; Butterfield, D. A. *Free Radical Biol. Med.* **2002**, *32*, 1205−1211.
(13) Chou, P. Y.; Fasman, G. D. *J. Mol. Biol.* **1977**, *115*, 135−175.
(14) Wood, S. J.; Wetzel, R.; Martin, J. D.; Hurle, M. R. *Biochemistry* **1995**, *34*, 724−730.
(15) Morimoto, A.; Irie, K.; Murakami, K.; Masuda, Y.; Ohigashi, H.; Nagao, M.; Fukuda, H.; Shimizu, T.; Shirasawa, T. *J. Biol. Chem.* **2004**, *279*, 52781−52788.
(16) Williams, A. D.; Portelius, E.; Kheterpal, I.; Guo, J.; Cook, K. D.; Xu, Y.; Wetzel, R. *J. Mol. Biol.* **2004**, *335*, 833−842.
(17) Murakami, K.; Irie, K.; Morimoto, A.; Ohigashi, H.; Shindo, M.; Nagao, M.; Shimizu, T.; Shirasawa, T. *Biochem. Biophys. Res. Commun.* **2002**, *294*, 5−10.
(18) Murakami, K.; Irie, K.; Morimoto, A.; Ohigashi, H.; Shindo, M.; Nagao, M.; Shimizu, T.; Shirasawa, T. *J. Biol. Chem.* **2003**, *278*, 46179−46187.
(19) Shao, H.; Jao, S.; Ma, K.; Zagorski, M. G. *J. Mol. Biol.* **1999**, *285*, 755−773.
(20) Coles, M.; Bicknell, W.; Watson, A. A.; Fairlie, D. P.; Craik, D. J. *Biochemistry* **1998**, *37*, 11064−11077.
(21) Petkova, A. T.; Ishii, Y.; Balbach, J. J.; Antzutkin, O. N.; Leapman, R. D.; Delaglio, F.; Tycko, R. *Proc. Natl. Acad. Sci. U.S.A.* **2002**, *99*, 16742−16747.
(22) Antzutkin, O. N.; Leapman, R. D.; Balbach, J. J.; Tycko, R. *Biochemistry* **2002**, *41*, 15436−15450.
(23) Petkova, A. T.; Leapman, R. D.; Guo, Z.; Yau, W. M.; Mattson, M. P.; Tycko, R. *Science* **2005**, *307*, 262−265.
(24) Irie, K.; Oie, K.; Nakahara, A.; Yanai, Y.; Ohigashi, H.; Wender, P. A.; Fukuda, H.; Konishi, H.; Kikkawa, U. *J. Am. Chem. Soc.* **1998**, *120*, 9159−9167.
(25) Carpino, L. A. *J. Am. Chem. Soc.* **1993**, *115*, 4397−4398.

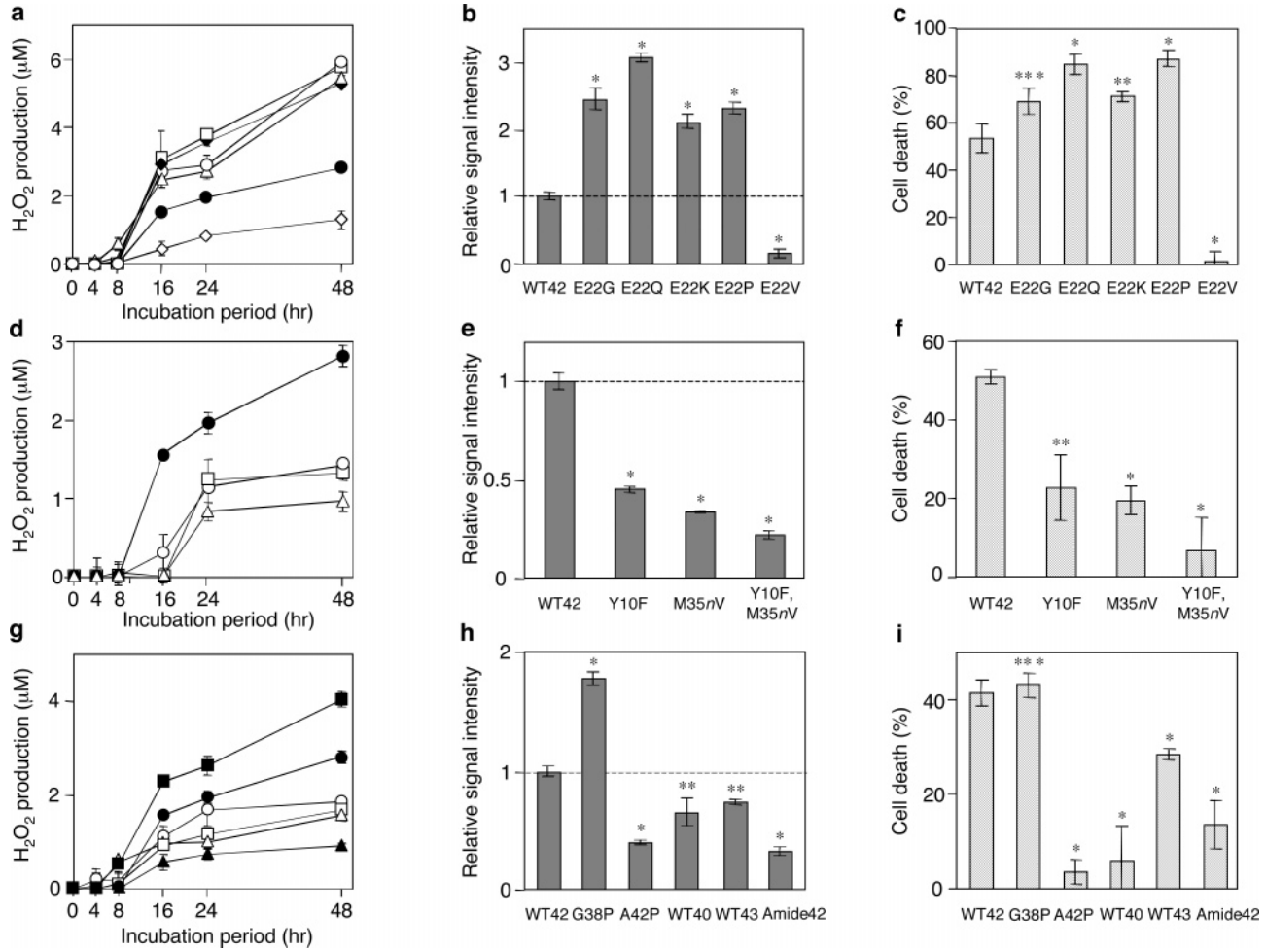


***Figure 2.*** Production of hydrogen peroxide and radicals by A$\beta$ mutants along with neurotoxicity in vitro. (a) Production of $H_2O_2$ by A$\beta$42 mutants substituted at position 22: ●, wild-type A$\beta$42; □, E22K−A$\beta$42; ◆, E22Q−A$\beta$42; ○, E22G−A$\beta$42; △, E22P−A$\beta$42; ◇, E22V−A$\beta$42. (b) A$\beta$42 mutants substituted at position 22 were examined for their ability to produce radicals originating from the hydroxyl radical as estimated by ESR spectrometry using PBN as a trapping reagent after a 48-h incubation. (c) Neurotoxicity of the CAA-related A$\beta$42 estimated with the MTT assay using PC12 cells. In the neurotoxicity assay, the concentration of each A$\beta$42 mutant was $10^{-6}$ M, which is close to the $IC_{50}$ value of wild-type A$\beta$42. (d) Production of $H_2O_2$ by Y10F−A$\beta$42, M35*n*V−A$\beta$42, and Y10F, M35*n*V−A$\beta$42: ●, wild-type A$\beta$42; ○, Y10F−A$\beta$42; □, M35*n*V−A$\beta$42; △, Y10F, M35*n*V−A$\beta$42. (e) Production of radicals by Y10F−A$\beta$42, M35*n*V−A$\beta$42, and Y10F, M35*n*V−A$\beta$42 after a 24-h incubation. (f) Neurotoxicity of Y10F−A$\beta$42, M35*n*V−A$\beta$42, and Y10F, M35*n*V−A$\beta$42. The concentration of each A$\beta$42 mutant was $10^{-6.5}$ M, which is close to the $IC_{50}$ value of wild-type A$\beta$42. (g) Production of $H_2O_2$ by G38P−A$\beta$42, A42P−A$\beta$42, A$\beta$43, and A$\beta$42(amide): ●, wild-type A$\beta$42; △, wild-type A$\beta$40; ■, G38P−A$\beta$42; ▲, A42P−A$\beta$42; □, wild-type A$\beta$43; ○, A$\beta$42(amide). (h) Production of radicals by G38P−A$\beta$42, A42P−A$\beta$42, A$\beta$43, and A$\beta$42(amide) after a 48-h incubation. (i) Neurotoxicity of G38P−A$\beta$42, A42P−A$\beta$42, A$\beta$43, and A$\beta$42(amide). The concentration of each A$\beta$42 mutant was $10^{-6.5}$ M, which is close to the $IC_{50}$ value of wild-type A$\beta$42. All of the error bars represent the standard deviation. *, $p < 0.001$ versus wild-type, **, $p < 0.01$ versus wild type, ***, $p < 0.05$ versus wild type.

**Peptide Preparation.** Each A$\beta$ mutant except for A$\beta$42(amide) was synthesized in a stepwise fashion on 0.1 mmol of preloaded Fmoc-Ala-PEG-PS resin with a Pioneer peptide synthesizer using the Fmoc strategy as reported previously.[15,17,18,26] Fmoc-PAL-PEG-PS resin (Applied Biosystems) was used for the synthesis of A$\beta$42(amide). After completion of the chain elongation, each peptide-resin was treated with a mixture containing trifluoroacetic acid, 1,2-ethanedithiol, thioanisole, and *m*-cresol for final deprotection and cleavage from the resin. The crude peptide precipitated by diethyl ether was purified by HPLC under alkaline conditions. Lyophilization gave a corresponding pure A$\beta$ peptide, the purity of which was determined by HPLC (>98%). The total yields of the peptides were consequently between 2% and 26%, indicating that the average coupling yield of each condensation step was 95−98%. Molecular weights were confirmed by MALDI-TOF-MS. The difference between the calculated and theoretical molecular mass was less than one mass unit. A$\beta$43 was purchased from Peptide Institute (Osaka, Japan).

**In Vitro Hydrogen Peroxide Assay.** The production of $H_2O_2$ was quantified using a colorimetric $H_2O_2$ assay kit, BIOXYTECH $H_2O_2$-560, following the manufacturer's directions. Each A$\beta$ mutant dissolved at 165 $\mu$M in 5 mM sodium phosphate buffer (150 mM NaCl) was incubated at 37 °C for 4, 8, 16, 24, or 48 h. One hundred microliters of the solution was added to 1 mL of a color reagent containing xylenol orange in an acidic solution with sorbitol and ammonium iron sulfate, and the optical density was read at 560 nm. The background value without the peptides was subtracted.

**ESR Spectrometry.** A reliable method for estimating the ability to produce radicals of A$\beta$ peptides using ESR was developed by Butterfield's group.[11] Each A$\beta$ mutant (165 $\mu$M) was dissolved in 5 mM sodium phosphate buffer (150 mM NaCl) containing 50 mM PBN according to their protocol.[11] To suppress the effect of excess metal-catalyzed reactions, the buffer was stirred for 48 h at room temperature in the presence of Chelex-100 resin. The deferoxamine mesylate was dissolved at 2 mM in the buffer prior to addition of an A$\beta$ peptide. The resultant peptide solution was incubated at 37 °C for 24 or 48 h. Four hundred microliters of each solution was placed into an ESR flat cell at appropriate time points for ESR analysis. The ESR spectrometry

(26) Morimoto, A.; Irie, K.; Murakami, K.; Ohigashi, H.; Shindo, M.; Nagao, M.; Shimizu, T.; Shirasawa, T. *Biochem. Biophys. Res. Commun.* **2002**, *295*, 306−311.

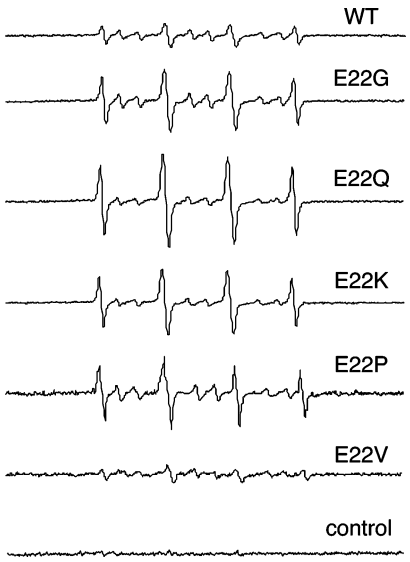


***Figure 3.*** ESR spectra of Aβ42 mutants altered at position 22 after a 48-h incubation at 37 °C.

was performed on an EMX ESR spectrometer at room temperature or 37 °C. Instrumental parameters were as follows: microwave power, 20 mW; microwave frequency, 9.8 GHz; modulation frequency, 100 kHz; modulation amplitude, 1.0 G; conversion time, 40.96 ms; scans, 100 (room temperature) or 200 (37 °C). Integral calculation of the radical intensity was performed after subtraction of the background spectrum.

**Estimation of Cell Survival.** The mitochondrial function in rat pheochromocytoma PC12 cells was evaluated using the MTT reduction assay as an indirect measure of cell viability.[27] We used PC12 cells to evaluate the cytotoxicity of Aβ peptide because PC12 cells, which have potential to differentiate into neural cells, are sensitive to Aβ peptides and are generally used for detecting cytotoxicity as a neurotoxicity model.[27] After a 48-h incubation with Aβ42 mutants, the rate at which formazan was produced was evaluated by measuring the optical density at 600 nm. The experimental procedure used is described elsewhere.[15,17,18,26] Data are given as percentages of the control values.

**Aggregation Test.** The aggregation kinetics of each Aβ mutant was estimated with the sedimentation assay using HPLC. The experimental procedure used is described elsewhere.[15,17,18,26] The area of absorption at 220 nm was integrated and expressed as a percentage of the control. The thermodynamic stability of Aβ fibrils was evaluated by the method of Williams et al.[16] The molar concentration of soluble Aβ peptides present at equilibrium was measured using a Micro BCA protein assay following the manufacturer's directions.

## Results and Discussion

**Estimation of Oxidative Stress of CAA-Related Aβ42 Mutants.** Our recent studies[17,18] revealed that the turn at positions 22 and 23 plays a critical role in the Aβ42-induced neurotoxicity. To investigate the effects of the turn on the formation of free radicals, the level of $H_2O_2$ produced by the CAA-related Aβ42 mutants altered at position 22 (E22K, E22Q, and E22G) together with E22P−Aβ42 and E22V−Aβ42 was measured. As shown in Figure 2a, E22K−, E22Q−, E22G−, and E22P−Aβ42 produced twice more $H_2O_2$ than wild-type Aβ42. In contrast, E22V−Aβ42 generated less $H_2O_2$ than the wild type. We also estimated levels of free radicals using ESR spectrometry with PBN as a trapping reagent (Figure 2b). After a 48-h incubation in the dark at 37 °C, all of the mutants except for E22V−Aβ42 produced stronger signals than wild-type Aβ42, the predominant shape of which was four-line (Figure 3). The shape of the spectra was equal to that of Butterfield's group,[11] but was different from that of Mason's group[28] and Allsop's group,[29] due to various factors such as the purity of the Aβ peptides and PBN, the incubation time, the light intensity, and so on. There was a good correlation among the production of $H_2O_2$, the formation of radicals, and the neurotoxicity in PC12 cells (Figure 2a−c), indicating that the turn at positions 22 and 23 of Aβ42 is indispensable for the neurotoxicity through the formation of radicals. Supporting this conclusion, we have recently verified the existence of a turn at positions 22 and 23 in the fibrils of E22K−Aβ42 with potent neurotoxicity using solid-state NMR.[30]

**Estimation of Oxidative Stress and Neurotoxicity of Aβ42 Mutants Altered at Positions 10 and 35.** The phenol hydroxyl group of Tyr-10 is easily oxidized through metal ions to give a tyrosyl radical.[31] The *S*-oxidized radical cation of Met-35 is also involved in the neurotoxicity.[5] However, the mechanism of its formation at a molecular level has not fully been clarified. The turn at positions 22 and 23 in Aβ42 might cause the tyrosyl radical at position 10 to interact with the sulfur atom of Met-35 to give the *S*-oxidized radical cation.

To investigate the contribution of Tyr-10 and Met-35 to the generation of free radicals and neurotoxicity, the amount of radicals produced by Y10F−Aβ42 and M35*n*V−Aβ42 together with their double mutant (Y10F, M35*n*V−Aβ42) was examined. Norvaline (*n*V) was selected because a methyl group has hydrophobicity quite similar to that of an *S*-methyl group. As shown in Figure 2d, Y10F−Aβ42, M35*n*V−Aβ42, and Y10F, M35*n*V−Aβ42 produced fairly low levels of $H_2O_2$ as compared to wild-type Aβ42. ESR measurements also showed that all of the mutations reduced the signal intensity of radicals after a 24-h incubation (Figure 2e). Their neurotoxic effects on PC12 cells also decreased significantly as shown in Figure 2f, indicating that both the tyrosyl and the methionine radicals could play a critical role in the radical-mediated neurotoxicity of Aβ42.

These results along with the propensity to form a turn at positions 22 and 23 in Aβ42 support the hypothesis that the tyrosyl radical could be reduced by the sulfur atom of Met-35, generating the *S*-oxidized radical cation that could extract activated hydrogens, leading to the formation of peroxyl radicals in the fatty acyl chains in phospholipids, eventually followed by the damage of membrane constituents as Butterfield proposed.[9,11] Kadlcik et al.[32] recently reported that the *S*-oxidized radical cation of Met-35 could cause the neurotoxic effect, while the tyrosyl radical of Tyr-10 could not, using pulse radiolysis. This result does not contradict our proposition that accessibility of Tyr-10 to Met-35 through the turn at positions 22 and 23 is essential to the neurotoxicity of Aβ42.

However, the *S*-oxidized radical cation is too short-lived to effectively cause such oxidative stress.[9] Quite recent research

(27) Shearman, M. S.; Ragan, C. I.; Iversen, L. L. *Proc. Natl. Acad. Sci. U.S.A.* **1994**, *91*, 1470−1474.
(28) Dikalov, S. I.; Vitek, M. P.; Maples, K. R.; Mason, R. P. *J. Biol. Chem.* **1999**, *274*, 9392−9399.
(29) Turnbull, S.; Tabner, B. J.; El-Agnaf, O. M. A.; Twyman, L. J.; Allsop, D. *Free Radical Biol. Med.* **2001**, *30*, 1154−1162.
(30) Masuda, Y.; Irie, K.; Murakami, K.; Ohigashi, H.; Ohashi, R.; Takegoshi, K.; Shimizu, T.; Shirasawa, T. *Bioorg. Med. Chem.* **2005**, *13*, in press.
(31) Ali, F. E.; Separovic, F.; Barrow, C. J.; Cherny, R. A.; Fraser, F.; Bush, A. I.; Masters, C. L.; Barnham, K. J. *J. Pept. Sci.* **2005**, *11*, 353−360.
(32) Kadlcik, V.; Sicard-Roselli, C.; Mattioli, T. A.; Kodicek, M.; Houee-Levin, C. *Free Radical Biol. Med.* **2004**, *37*, 881−891.

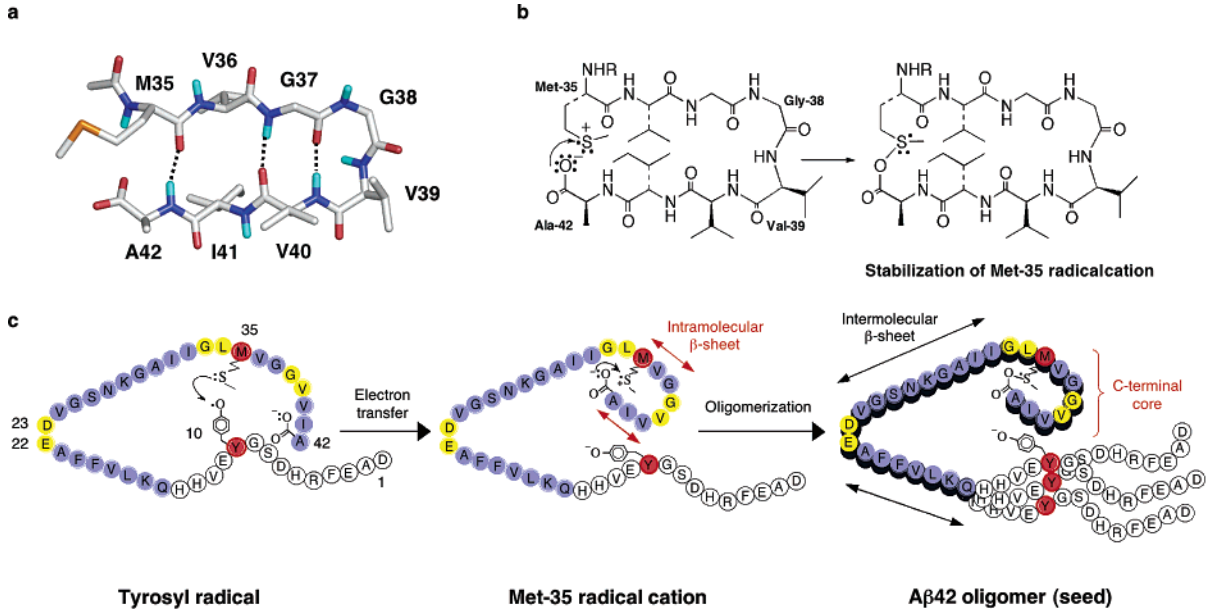


***Figure 4.*** Possible mechanism stabilizing the radical species derived from A$\beta$42. (a) The intramolecular antiparallel $\beta$-sheet at the C-terminus of A$\beta$42. The dotted lines indicate hydrogen bonds. (b) Possible participation of the group neighboring the C-terminal carboxylate anion in A$\beta$42. Our proline scanning data[15] strongly support this mechanism. (c) New mechanism of A$\beta$42-induced neurotoxicity based on our fibrillar model of A$\beta$42 with systematic proline replacement.[15] By chelating trace amounts of metal ions at the N-terminal histidines, the A$\beta$42 monomer would generate $H_2O_2$, leading to the oxidation of the phenol hydroxyl group at position 10. The turn structure at positions 22 and 23 would bring the resultant tyrosyl radical close to the sulfur atom of Met-35 to produce the *S*-oxidized radical cation, which could be stabilized by the C-terminal carboxylate anion through the intramolecular $\beta$-sheet. The C-terminal core would induce aggregation of A$\beta$42 to confine the radical species to oligomers that would release the radicals continuously through equilibration with the monomer. This mechanism explains well the long-term oxidative damage of the oligomers and/or fibrils of A$\beta$42. Because such a mechanism is not possible in A$\beta$40, its neurotoxic effects would be extremely weak. Almost all of the A$\beta$42 except for the oligomer as a seed might form an intermolecular parallel $\beta$-sheet structure in the C-terminus as Török et al. proposed.[40]

using D1M−A$\beta$42,[33] in which methionine was substituted for Asp-1 and all subsequent residues from Asp-1 to Leu-34 were shifted one position toward the C-terminus to mimic the neurotoxic and radical-generating effects of A$\beta$42, suggested that the *S*-oxidized radical cation could be stabilized by the N-terminal nitrogen to yield an N−S radical cation.[34] There must be a similar mechanism of stabilization of the methionine radical by a neighboring group in the case of the wild-type A$\beta$42.

**Estimation of Oxidative Stress and Neurotoxicity of A$\beta$42 Mutants Altered at the C-Terminus.** Our recent research[15,26] based on the systematic replacement of prolines in A$\beta$42 revealed that the C-terminal structure contains two $\beta$-sheet regions at positions 35−37 and 40−42 separated by a turn at positions 38 and 39 (Figure 1a). G38P−A$\beta$42 with strong aggregative ability produced more radicals than wild-type A$\beta$42, while A42P−A$\beta$42 without aggregative ability showed a decrease in radical-generating activity (Figure 2g,h), strongly supporting the contribution of the turn at positions 38 and 39 to the neurotoxicity through the generation of radicals. The turn at positions 38 and 39 suggests the formation of an intramolecular antiparallel $\beta$-sheet at positions 35−42, enabling the association of the sulfur atom of Met-35 with the C-terminal carboxylate anion to stabilize the methionine radical (Figure 4a). To verify this assumption, A$\beta$42(amide), in which the C-terminal carboxylic acid is converted into an amide, was examined for its ability to generate radicals and its neurotoxicity. As shown in Figure 2g and h, the production of $H_2O_2$ and formation of radicals induced by A$\beta$42(amide) decreased significantly. A$\beta$42(amide) also showed less neurotoxicity than wild-type A$\beta$42 (Figure 2i). These results strongly suggest that interaction of the C-terminal carboxylate anion with the *S*-oxidized radical cation of Met-35 through the intramolecular antiparallel $\beta$-sheet could be essential to the neurotoxicity of A$\beta$42 (Figure 4a,b). In the case of A$\beta$40, the *S*-oxidized radical cation of Met-35 would not be fully stabilized, resulting in a less neurotoxic effect because there is no such neighboring interaction at the C-terminus of A$\beta$40. Moreover, A$\beta$43, which occurs occasionally,[2] also produced fewer radicals and was less neurotoxic (Figure 2g−i), indicating that the C-terminal length of A$\beta$42 is important for neurotoxicity through the stabilization of radicals.

Kanski et al.[12] reported that the backbone carbonyl function of Ile-31 in the α-helix environment would lead to interaction with the sulfur atom of Met-35, to result in the one-electron oxidation of the sulfur atom, generating the *S*-oxidized radical cation. Because prolines are rarely found in α-helix as well as $\beta$-sheet,[13] their data do not contradict the results of systematic proline replacement.[15] They also proposed that the Gly centered radicals at positions 29 and 33 could be involved in the stabilization of the *S*-oxidized radical cation.[35] This hypothesis was verified by the theoretical calculations (an ONIOM study) of Brunelle and Rauk.[36] The specific association of Gly-29 and Gly-33 with Met-35 is consistent with our model of the aggregation of A$\beta$42 containing the turn at positions 33 and 34 (Figure 1a). However, this mechanism of stabilization seems to be more important in A$\beta$40 than in A$\beta$42.

**Effect of Radical Productivity on Aggregative Ability.** There exists a good correlation between the neurotoxicity in

(33) Boyd-Kimball, D.; Sultana, R.; Mohmmad-Abdul, H.; Butterfield, D. A. *Peptides* **2005**, *26*, 665−673.
(34) Miller, B. L.; Kuczera, K.; Schöneich, C. *J. Am. Chem. Soc.* **1998**, *120*, 3345−3356.
(35) Kanski, J.; Varadarajan, S.; Aksenova, M.; Butterfield, D. A. *Biochim. Biophys. Acta* **2001**, *1586*, 190−198.
(36) Brunelle, P.; Rauk, A. *J. Alzheimer's Dis.* **2002**, *4*, 283−289.

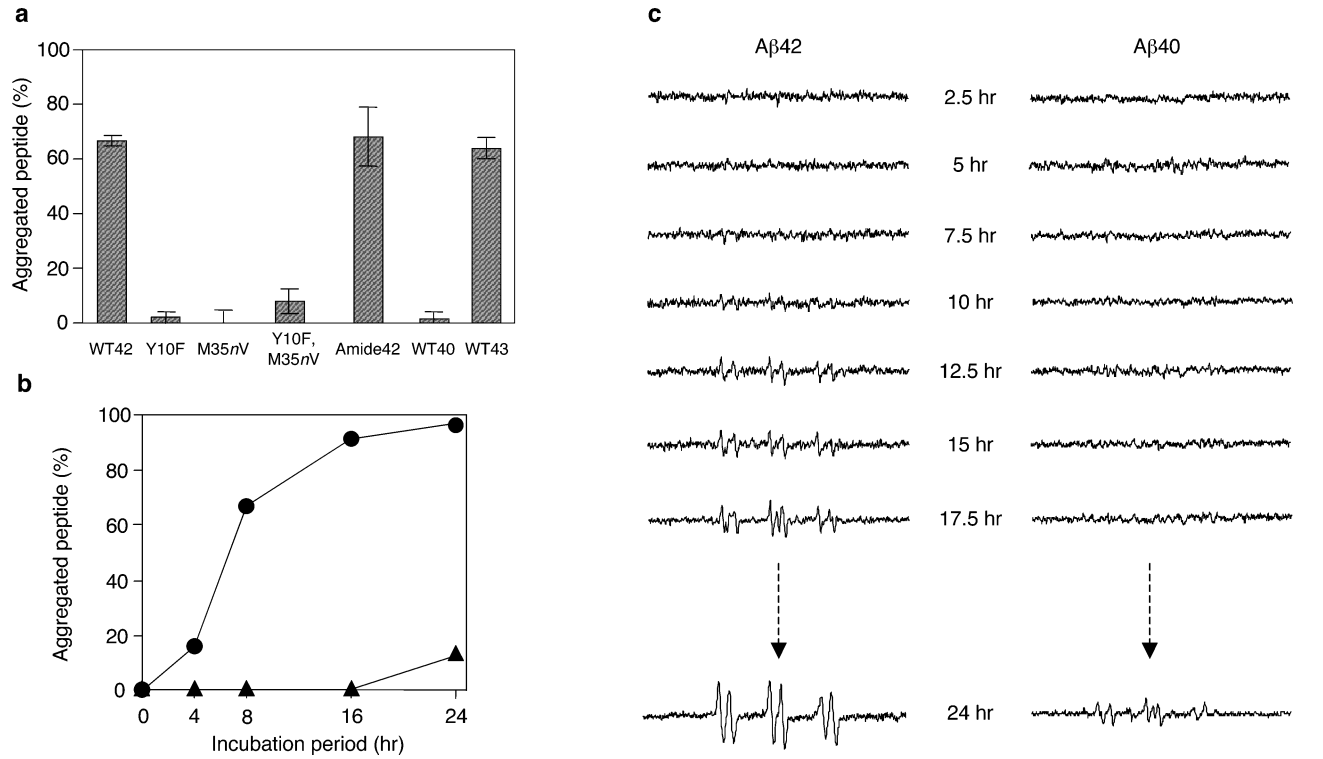


***Figure 5.*** Aggregation kinetics and production of radicals by A$\beta$ peptides. (a) The aggregation kinetics of A$\beta$ mutants was estimated using the sedimentation assay. The bar shown represents the amount of aggregated peptides after an 8-h incubation at 37 °C. (b) Aggregation velocity of A$\beta$42 and A$\beta$40: ●, wild-type A$\beta$42; ▲, wild-type A$\beta$40. (c) ESR spectrometry was performed at 37 °C continuously. The spectra of A$\beta$42 (left) and A$\beta$40 (right) were recorded at 2.5, 5, 7.5, 10, 12.5, 15, 17.5, and 24 h, respectively. The background spectrum without the peptides was subtracted in the spectra shown. The reverse peptide of A$\beta$1−40 (A$\beta$40−1) is reported to show almost no signal.[28]

PC12 cells and the aggregation kinetics of the A$\beta$ mutants.[15,17,18,26] However, it is not known how the aggregation is related to neurotoxicity through the formation of radicals. Atwood et al.[8] recently reported that the oligomerization of A$\beta$ peptides is initiated by dityrosine cross-linking through the interaction of $H_2O_2$ with a Cu(II) tyrosinate. To investigate the relationship between the ability to produce radicals and to aggregate, all of the mutants with substitutions at positions 10, 35, and 42 in Figure 2 were examined for their aggregative ability by the sedimentation assay: HPLC analysis after centrifugation of the A$\beta$ solution (Figure 5a). Only the results of the sedimentation assay are shown because the HPLC data are more reliable than the Th-T fluorescence data as reported previously.[18] Y10F−, M35*n*V−, and Y10F, M35*n*V−A$\beta$42 showed a slower aggregation kinetics than wild-type A$\beta$42, suggesting that both the tyrosyl radical at position 10 and the *S*-oxidized radical cation of Met-35 play a significant role in the aggregation of A$\beta$42. Although A$\beta$42(amide) and A$\beta$43 showed a kinetics comparable to wild-type A$\beta$42, their molar concentrations of soluble A$\beta$ peptides present at equilibrium ($2.2 \pm 0.088$ and $2.3 \pm 0.10$ $\mu$M, respectively) were higher than that of wild-type A$\beta$42 ($0.85 \pm 0.035$ $\mu$M), suggesting that their fibrils exhibited less thermodynamic stability than those of wild-type A$\beta$42 by 0.6 kcal/mol. These results indicate that a S−O bond between the *S*-oxidized radical cation of Met-35 and the carboxylate anion of Ala-42 could make an oligomer of A$\beta$42 highly stable (Figure 4b). We are trying to obtain evidence of the formation of a S−O bond in the C-terminal core.

**Time-Course Analysis of Radical Production.** According to our C-terminal model (Figure 4a,b), only A$\beta$42 can deposit effectively the methionine radicals in the oligomers and/or fibrils, inducing longer-lasting damage to cells through equilibration with the monomer. To test this hypothesis, we continuously measured the amount of radicals generated by A$\beta$42 and A$\beta$40 using ESR in the presence of light at 37 °C, where six-line spectra were dominant. As shown in Figure 5c, detectable levels of A$\beta$42 were observed only after a 12.5-h incubation, and the intensity increased to reach a plateau after a 24-h incubation. More than 90% of A$\beta$42 had aggregated after a 16-h incubation even at a lower concentration (25 $\mu$M) than that in the ESR measurement (165 $\mu$M) in Figure 5b, suggesting that A$\beta$42 aggregates (oligomers) would release radicals after aggregating. On the other hand, A$\beta$40 did not show a significant level of radical production even after a 24-h incubation (Figure 5c). In the cytotoxicity assay, the neurotoxicity of A$\beta$40 was extremely low (Figure 2i). Because A$\beta$40 at 25 $\mu$M did not aggregate sufficiently after a 24-h incubation (Figure 5b), A$\beta$40 would not be able to stabilize the radicals by forming oligomers and/or fibrils resulting in low neurotoxicity as compared to A$\beta$42.

## Conclusions

On the basis of these results, we propose a new model for the aggregation of A$\beta$42 to explain its potent neurotoxicity as shown in Figure 4c. A$\beta$42 generates $H_2O_2$ in collaboration with metal ions, leading to the oxidation of Tyr-10. The formation of a turn at positions 22 and 23 would bring the resultant tyrosyl radical at position 10 in close proximity to the sulfur atom of Met-35 to produce the *S*-oxidized radical cation, which could be stabilized by a C-terminal core formed by the intramolecular $\beta$-sheet at positions 38 and 39. The C-terminal core would

accelerate the aggregation, leading to the oligomer (seed) and/or fibrils that could confine the radical species to result in a long-lasting oxidative stress on A$\beta$42 through equilibration with the monomer. Oligomers (dimers or trimers) of A$\beta$ aggregates might be more neurotoxic than fibrils in the etiology of AD.[37,38] Weinreb et al.[39] proposed "the hypothesis of hydrophobic cluster", stating that hydrophobic interaction among the side chains at the C-terminus caused by the formation of a turn at positions 37 and 38 of A$\beta$ peptides induces aggregation. Our model including turn at positions 38 and 39 at the C-terminus would be more reasonable for enabling the association of the sulfur atom of Met-35 with the C-terminal carboxylate anion to stabilize the methionine radical. Our new model also suggests that the formation of A$\beta$ radicals would be indispensable for their aggregation as well as neurotoxicity, and could also explain clearly the difference in aggregative ability and neurotoxicity between A$\beta$42 and A$\beta$40 at the molecular level, leading to unique opportunities to design antibodies and inhibitors that are specific to the malignant conformation of A$\beta$42 (Figure 1a), such as the turns at positions 22 and 23, and 38 and 39. However, the mutation of A$\beta$42 might cause the conformational change, and an alternative explanation for the present results is possible. Caution should be used for the model presented in this work until the crystal structure of A$\beta$42 aggregates is clarified by X-ray analysis.

**Acknowledgment.** We thank Dr. Hiroyuki Fukuda of Applied Biosystems Japan, Ltd., for MALDI-TOF-MS measurements. This research was supported in part by Grants-in-aid for Scientific Research (B) (No. 13460048 and 16380080 to K I.) and for Scientific Research on Priority Areas (No. 17025051 to T.Shim., T.Shir., and K.I.), Special Coordination Funds (to H.O.), and a Grant-in-aid for the Promotion of Science for Young Scientists (No. 16.1215 to K. M.) from the Ministry of Education, Culture, Sports, Science, and Technology of the Japanese Government.

**Supporting Information Available:** MALDI-TOF-MS data on Y10F−A$\beta$42, M35*n*V−A$\beta$42, Y10F, M35*n*V−A$\beta$42, and A$\beta$42(amide). This material is available free of charge via the Internet at http://pubs.acs.org.

JA054041C

(37) Bucciantini, M.; Giannoni, E.; Chiti, F.; Baroni, F.; Formigli, L.; Zurdo, J.; Taddei, N.; Ramponi, G.; Dobson, C. M.; Stefani, M. *Nature* **2002**, *416*, 507−511.
(38) Walsh, D. M.; Klyubin, I.; Fadeeva, J. V.; Cullen, W. K.; Anwyl, R.; Wolfe, M. S.; Rowan, M. J.; Selkoe, D. J. *Nature* **2002**, *416*, 535−539.
(39) Weinreb, P. H.; Jarrett, J. T.; Lansbury, P. T., Jr. *J. Am. Chem. Soc.* **1994**, *116*, 10835−10836.
(40) Török, M.; Milton, S.; Kayed, R.; Wu, P.; McIntire, T.; Glabe, C. G.; Langen, R. *J. Biol. Chem.* **2002**, *277*, 40810−40815.